Phonon renormalization effects in quantum wells

S. Das Sarma and M. Stopa
Department of Physics and Astronomy, University of Maryland, College Park, Maryland 20742
(Received 2 July 1987)

We investigate the effects of screening on polaronic corrections to the effective band edge and effective mass in a quasi-two-dimensional GaAs quantum well. We find that both screening and finite well width significantly reduce the polaron energy and thus oppose the polaronic band-gap renormalization. We calculate how this "counter-renormalization" depends on the free-carrier density and temperature. We show that static screening overestimates screening in comparison with dynamical screening. We calculate the polaronic effective mass as a function of free-carrier density and temperature and show that the calculated temperature dependence of screening is too small to account for the observed temperature dependence in recent cyclotron resonance measurements of effective mass.

I. INTRODUCTION

The coupling between electrons and LO phonons in weakly polar semiconductor quantum wells affects the band-gap energy and the electronic effective mass. Individual (and hole) energies and consequently the energy gap between the valence and conduction bands are renormalized by the emission and absorption of LO phonons. Equivalently, one can picture the energy change as resulting from the polarization of the ions surrounding a given electron. Since electronic motion necessitates the polarization of the region into which the electron is moving (i.e., the electron must carry the phonon cloud with it), which requires energy, the effective mass of the polaron is greater than that of a bare electron.[1]

Screening by free carriers (electrons in the conduction band and/or holes in the valence band) serves to reduce the coupling between electrons (or holes) and LO phonons. The polaronic self-energy lowers the conduction band and raises the valence band, thereby narrowing the band gap. Thus screening, by reducing the magnitude of the polaronic self-energy, acts to oppose the renormalization and tends to widen the gap back to its unrenormalized bare value. This "counter-renormalization" is the central concern of this paper.

We calculate the polaronic band-edge renormalization for a GaAs-$Al_xGa_{1-x}As$ quantum well as a function of temperature and carrier density in this paper. The unrenormalized gap between the valence and conduction bands in bulk GaAs is roughly 1.5 eV. Our renormalization of the band gap due to LO-phonon coupling is of the order of 10 meV. This is comparable to the magnitude of exchange-correlation corrections to the band gap.[2] We also calculate the electronic effective mass correction due to the screened electron–LO-phonon interaction as a function of temperature, generalizing the earlier work of Das Sarma and Mason.[3] Our results are compared with recent cyclotron resonance experiments[4] on the electron effective mass in GaAs quantum wells.

Electron–LO-phonon coupling depends[5] upon well width, free-carrier density, and temperature, which we discuss in turn. The electronic wave function is quantized in the direction normal to the interface (the z direction). Free effective-mass-like motion is possible in the x-y plane. We ignore interface effects on phonons (i.e., we assume the lattices are well matched) and consider the coupling of electrons to bulk phonons. The quantized z-direction wave functions lead to a form factor[5–7] which modifies the otherwise two-dimensional interaction. This form factor, and hence the electronic self-energy, naturally depends on well width. We span the range of typical well widths by calculating energies and masses in wells from 0 to 400 Å.

We do not limit the phase space in the self-energy integral via a Fermi occupancy factor since the typical Fermi energy (E_F) is substantially less than the GaAs LO-phonon energy. We *do*, however, incorporate the effects of free-carrier density in screening since two-dimensional screening in the leading-order approximation is density independent. Typical densities are of the order of 10^{11} particles/cm^2. Our main interest in this paper is in studying the effects of carrier density, well width, and temperature on screening corrections to the renormalization of band edges and effective mass. Phonon occupancy and screening are both temperature dependent. We include the relevant Bose factors in the perturbative self-energy calculations.

We calculate the band-gap renormalization in two ways. The first calculation is the straightforward perturbative approach of evaluating the leading-order self-energy diagram. Since full dynamical screening in the perturbative calculation is intractable, we are forced to use static screening. Our second approach is to use a variational expression[8] involving the structure factor. This employs the dynamical dielectric function in the calculation of the screened electron-phonon interaction via the electronic structure factor. We have carried out the variational calculation at $T=0$ only.

II. PERTURBATIVE CALCULATION

A. Electron self-energy

The leading-order electron (hole)–LO-phonon self-energy (within a static screening approximation) is given

by[5]

$$\mathrm{Re}\Sigma_{\pm}(\mathbf{k},E)=\frac{\alpha_{\pm}\omega_{\mathrm{LO}}^{3/2}}{2\pi(2m_{\pm})^{1/2}}\int_0^{\infty}\frac{F(q)dq}{[\epsilon(q,0)]^2}\int_0^{2\pi}d\theta\left[\frac{n_0}{E+\omega_{\mathrm{LO}}-E_0(\mathbf{k}-\mathbf{q})}+\frac{1+n_0}{E-\omega_{\mathrm{LO}}-E_0(\mathbf{k}-\mathbf{q})}\right], \tag{2.1}$$

where $\alpha_{\pm}$ is the Fröhlich coupling constant and equals 0.07 for electrons and approximately 0.192 for holes, ω_{LO} is the LO-phonon energy and equals 36.5 meV, $m_{\pm}$ is the bare-hole (electron) band mass, n_0 the Bose occupancy factor, and $E_0(\mathbf{k}-\mathbf{q})$ the bare-electron energy. We take $0.067m_0$ as our bare (band) mass for the electron and $0.50m_0$ for holes. If we assume only the lowest subband is occupied, we have the form factor[5]

$$F(q)=8(q^2a^2+4\pi^2)^{-1}\left[\tfrac{3}{8}qa+\frac{\pi^2}{qa}-\frac{4\pi^4}{q^2a^2}(q^2a^2+4\pi^2)^{-1}(1-e^{-qa})\right], \tag{2.2}$$

where a is the well width. We approximate the quantum well by an infinite square-well potential of width a which is known to be a fairly good approximation in the electric quantum limit with only the lowest subband occupied. We assume a static random-phase approximation (RPA) for the dielectric function:[9]

$$\epsilon(q,E=0,T)=1+\frac{q_{\mathrm{TF}_+}(q)}{q}+\frac{q_{\mathrm{TF}_-}(q)}{q}, \tag{2.3}$$

where

$$q_{\mathrm{TF}_{\pm}}(q)=\left[q_{s_{\pm}}\int_0^{0.25}dx\frac{1-\tanh(Ax-\delta)}{(1-4x)^{1/2}}\right]F(q), \tag{2.4}$$

where $q_{s_{\pm}}=2m_{\pm}e^2/\kappa$, $A=\beta q^2/4\pi m_{\pm}$, $\beta=1/k_BT$, $\delta=\ln(e^{\beta k_F^2/2m}-1)/2\pi$, k_F is the Fermi wave vector equal to $(2\pi N_s)^{1/2}$. We take κ, the static dielectric constant, to be 12.5. Temperature enters the theory through the chemical potential and the screening function as shown above.[9]

Several assumptions underlie Eq. (2.1). They are as follows. (1) Electron-phonon coupling is given by the Fröhlich Hamiltonian. (2) Any dispersion in the phonon energy is negligible. (3) The electron can be described by a bare propogator, rather than solving Dyson's equation self-consistently. (4) As discussed in the Introduction, we have assumed a single particle in a subband by neglecting Fermi statistics, but we maintain a free-carrier density dependence in the screening (this is the usual "polaron" limit).

We are at liberty to consider screening by both electrons and holes, as is appropriate for a photoexcited intrinsic semiconductor; or by holes only for hole energies and electrons only for electron energies, as is appropriate for doped p- and n-type semiconductors, respectively. We will usually take the latter approach for purposes of comparison with our variational calculations (Sec. III).

We take the usual parabolic form of the electron energy: $E_0=k^2/2m$. We note that certain compound semiconductors (e.g., InSb) can be quite nonparabolic and would require that we keep higher-order corrections[10] to the bare energy. In addition, we consider electrons on the mass shell ($E\cong k^2/2m$). Thus, we obtain

$$\mathrm{Re}\Sigma_{\pm}(\mathbf{k},E)=\frac{a_{\pm}\omega_{\mathrm{LO}}^{3/2}}{2\pi(2m)^{1/2}}\int_0^{\infty}dq\int_0^{2\pi}d\theta\left[\frac{n_0}{\omega_{\mathrm{LO}}-q^2/2m+kq\cos\theta/m}+\frac{1+n_0}{-\omega_{\mathrm{LO}}-q^2/2m+kq\cos\theta/m}\right]\frac{F(q)}{[\epsilon(q,0)]^2}. \tag{2.5}$$

Finally, since we are interested in the band edge, we set $k=0$ and perform the angular integration to get the following results for the polaronic corrections $\epsilon_{p\pm}$ to the band edges:

$$\epsilon_{p\pm}\equiv\mathrm{Re}\Sigma_{\pm}(0,0)=\frac{\alpha_{\pm}\omega_{\mathrm{LO}}^{3/2}}{(2m)^{1/2}}\int_0^{\infty}dq\left[\frac{n_0}{\omega_{\mathrm{LO}}-q^2/2m}-\frac{1+n_0}{\omega_{\mathrm{LO}}+q^2/2m}\right]\frac{F(q)}{[\epsilon(q,0)]^2}. \tag{2.6}$$

In the limit where $F \to 1$ (strictly two-dimensional well) and $\epsilon \to 1$ (no screening), we have $\epsilon_{p\pm} \to \pi\alpha_{\pm}\omega_{\rm LO}/2$. This is about 4 meV for electrons and 10 meV for holes in a GaAs structure.

B. Effective mass

The definition for the polaron effective mas is

$$\frac{1}{m^*} = \lim_{k\to 0} \frac{1}{k} \frac{\partial E_p(k)}{\partial k} = \frac{1}{m} + \lim_{k\to 0} \frac{1}{k} \frac{\partial}{\partial k} \mathrm{Re}\Sigma(\mathbf{k},E) , \tag{2.7}$$

where $E_p(k) = (k^2/2m) + \mathrm{Re}\Sigma(k, k^2/2m)$ is the polaron dispersion. For low temperatures ($T \lesssim 50$ K) the phonon occupancy is negligible. Taking $n_0 \to 0$ in Eq. (2.5), we expand the remaining integrand in powers of k, take the k derivative, and perform the angular integration. Letting $k \to 0$ once more, we obtain

$$\frac{1}{m^*} = \frac{1}{m} - \frac{\alpha}{m} \left[\frac{(\omega_{\rm LO}/m)^{3/2}}{(2)^{1/2}} \int_0^\infty dq \frac{F(q)}{[\epsilon(q,0)]^2} \times \frac{q^2}{[\omega_{\rm LO} + q^2/2m]^3} \right]$$

$$\equiv \frac{1}{m} - \frac{\alpha C}{m} , \tag{2.8}$$

where C is the quantity within large parentheses. In the weak-coupling limit we get $m^* = m(1+\alpha C)$. In the two-dimensional, zero-screening limit [$F(q) \to 1, \epsilon(q,0) \to 1$], this reduces to

$$\frac{1}{m^*} = \frac{1}{m}(1 - \pi\alpha/8) , \tag{2.9}$$

giving the well-known result $m^* \cong m(1+\pi\alpha/8)$ in the weak-coupling limit.

III. VARIATIONAL CALCULATION

The dynamical structure factor is the spectral function for the density-density correlation function in an electron gas. It is related to the dynamical dielectric function:

$$S(\mathbf{k},\omega) = \frac{1}{\pi v_k} \mathrm{Im} \left[\frac{-1}{\epsilon(\mathbf{k},\omega)} \right] . \tag{3.1}$$

Here, v_k is the Fourier transform of the Coulomb interaction. A variational expression for the polaron energy which allows us to take advantage of the dynamical response information contained in the structure factor has been derived[8,11] by Devreese *et al.* for a polaron gas. The corresponding two-dimensional result can be obtained in a straightforward manner:

$$\epsilon_{p\pm} = \frac{-\alpha_{\pm}\omega_{\rm LO}}{(2m_{\pm}\omega_{\rm LO})^{1/2}} \int_0^\infty dk \frac{[S(\mathbf{k})]^2}{S(\mathbf{k}) + (k^2/2m_{\pm}\omega_{\rm LO})} , \tag{3.2}$$

where

$$S(\mathbf{k}) = \frac{1}{N_s} \int_0^\infty d\omega\, S(\mathbf{k},\omega)$$

is the static structure factor (note that it is *not* the simple static limit of the dynamical structure factor). We employ different approximations for the static structure factor (frequency integral already performed) to test various screening results. The first is the simple Hartree-Fock approximation:[12]

$$S_{\rm HF}(k) = \begin{cases} (2/\pi)\sin^{-1}(k/2k_F) + (k/\pi k_F)[1-(k/2k_F)^2]^{1/2}, & k \le 2k_F \\ 1 \quad \text{otherwise} . \end{cases} \tag{3.3}$$

One should use the random-phase approximation[13] (RPA) for $\epsilon(k,\omega)$ to obtain the static structure factor by doing an integration over the frequency. An easier approximate expression for the structure factor is obtained by noting that for small k, plasmons dominate the structure factor, whereas for large k it must approach unity. In fact, for $k > k_c$ (where k_c is the critical wave vector for plasmon damping by electron-hole pair production) the main contribution to the structure factor comes from electron-hole pairs. Thus for large k ($k > 2k_F$), the Hartree-Fock form for the structure factor (which takes into account only the electron-hole pairs) should be approximately correct, whereas for small k ($< 2k_F$) the plasmon-pole form should suffice. This enables us to use the following plasmon-pole approximation for the static structure factor:

$$S(k) = \frac{k^2}{2m[ak + k^2 B^2(k)]^{1/2}} \quad \text{for all } k , \tag{3.4}$$

where

$$B^2(k) = \frac{B^2}{\{1 - \Theta(k-2k_F)[1-(2k_F/k)^2]\}^{1/2}}$$

with

$$B^2 = v_F^2/2 = \tfrac{1}{2}(k_F/m)^2$$

and

$$a = 2\pi N_s e^2/(\kappa m) .$$

Here, $\Theta(k-2k_F)$ is the step function. Screening here is incorporated through the zero-temperature Lindhard[14] function in $B^2(k)$. This plasmon-pole approximation for the dielectric function has been shown[15] to work extremely well for a two-dimensional electron gas and should be numerically equivalent to the full RPA.

IV. RESULTS

A. Static and dynamical screening ($T=0$)

In Figures 1(a) and 1(b) we show electron and hole band-edge polaronic corrections, respectively, in the zero-well-width limit as a function of free-electron density for each of our three approximations: the perturbative and the two variational methods. The completely unscreened polaron energy is indicated by a horizontal line at the bottom of each figure. There is considerable screening in all methods even for the lowest density which we consider ($\sim 10^{11}$ cm^{-2}). Nonetheless, all the curves approach the unscreened limit as the density vanishes.

We also note that static screening "counter-renormalizes" the band gap more strongly than dynamical screening. Since static screening only considers the long-time response of the system to external fields, we are not surprised that this approach tends to overestimate screening. The Hartree-Fock screening always underestimates screening effect and we do not show any additional result with this approximation.

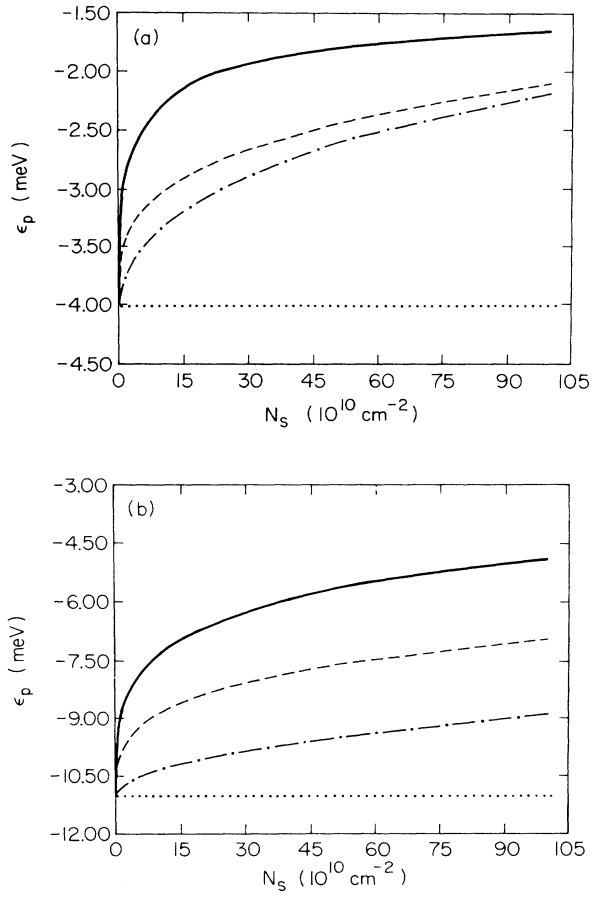

FIG. 1. Polaronic corrections (in the strictly two-dimensional zero-well-width limit) to the conduction-band edge (a) and valence-band edge (b) as a function of free-carrier density [electrons only in (a), holes only in (b)] for $T=0$, for three approximations: the perturbative calculation (solid lines), the variational calculation employing the plasmon pole structure factor (dashed lines), and the variational calculation employing the Hartree-Fock approximation for the structure factor (dash-dotted lines). The dotted lines denote the unscreened limits.

B. Well width

The effects of finite well thickness are dramatically apparent in Fig. 2(a) for the perturbative calculation and Fig. 2(b) for the dynamical variational calculation. In each of these figures the results for zero well thickness are replotted for comparison. Evidently, the polaron energy drops off very rapidly as the well increases from 0 Å (strictly two dimensions) to 100 Å. It continues to fall more slowly as the well thickness increases to 400 Å. Although the shapes of the curves for different well sizes are roughly the same, there is a tendency for higher densities to be slightly less affected by an increase in well width (say, from 0 to 100 Å) than lower densities. This can be seen by recognizing that at higher densities the self-energy depends more strongly on coupling with shorter wavelength (higher q) phonons; the others being screened out. The form factor for finite well thickness affects most strongly those short-wavelength phonons. In Fig. 2(c) we show the polaronic band-edge correction for the electrons in a photoexcited situation with equal number of electrons and holes in the perturbative static screening calculation. Figure 2(d) shows the corrections to the valence-band edge, with screening by holes only, in the dynamical variational calculation. Again the variation of the band edge with well width is most pronounced between 0 and 100 Å.

Figures 2 clearly indicate that finite well thickness affects the perturbative and variational calculations in much the same way, and typical conduction- and valence-band edges in GaAs quantum wells are shifted by polaronic corrections of the orders of 1–2 meV and 5–8 meV, respectively.

C. Temperature dependence (perturbative calculation)

Figure 3 shows the effects of finite temperature on the electron self-energy. In Fig. 3(a) we show the conduction-band correction as a function of free-carrier density for a variety of temperatures in the strictly two-dimensional zero-well-width limit. Figure 3(b) shows the same curves for a well whose width is 200 Å. The overall trend is clearly for the self-energy to decrease (increase in magnitude) as temperature increases. The zero-temperature curve is everywhere above the 25-K curve. Nonetheless, when we plot electron energy versus temperature for a variety of densities in Fig. 4, we see some slight structure at low temperatures. Again Figs. 4(a) and 4(b) differ in well width only. Figure 4(a) is the zero-width limit and Fig. 4(b) is 100 Å this time. Evidently, there is some competition between effects to increase and to decrease the self-energy at very low temperatures.

This phenomenon is easily explained physically. As we explain in Sec. I the effect of temperature is twofold.

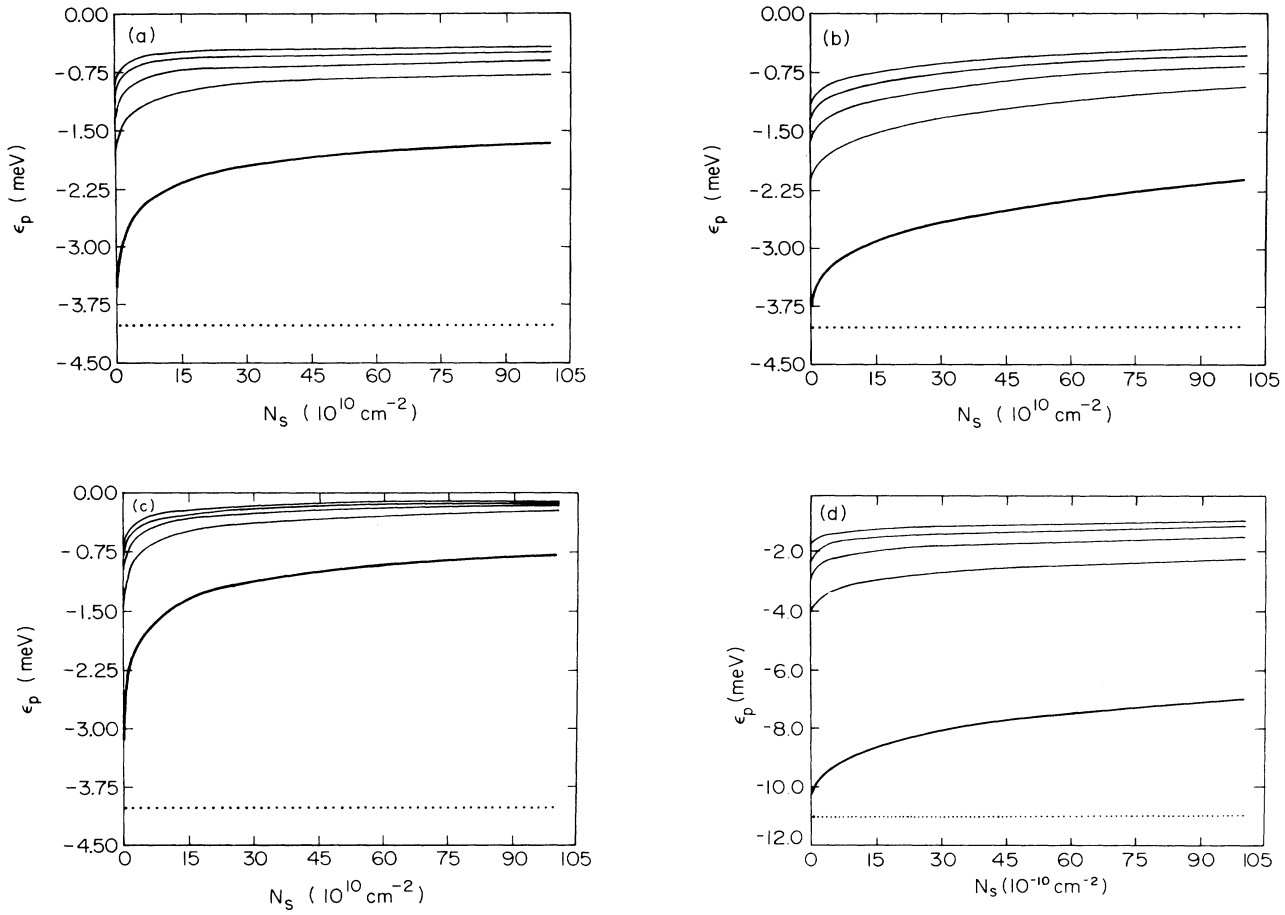

FIG. 2. Polaronic corrections (at $T=0$) to the band edges for a variety of well widths as a function of free-carrier density. (a) shows the perturbative corrections to the conduction-band edge with screening by electrons only. (b) shows the variational calculation corrections to the conduction-band edge with screening by electrons only. (c) shows the perturbative corrections to the conduction-band edge with screening by an equal number of holes and electrons. (d) shows the variational calculation corrections to the valence-band edge with screening by holes only. The thick curves are for the two-dimensional zero-well-width limit. The other well widths are, from bottom to top, 100, 200, 300, and 400 Å. The horizontal dotted lines indicate the completely unscreened, zero-width limits.

First, the self-energy at $T=0$ is due entirely to virtual phonons (there are no real phonons). As we move to room temperature we obtain a small but finite number of real phonons. But the emission and absorption of these phonons makes a relatively small contribution to the self-energy even at these higher temperatures—amounting to no more than 10% of the self-energy at 300 K. For the most part, the dependence of self-energy on density and temperature merely reflects the dependence of screening on temperature and wavelength. Intuitively, we expect screening to decrease as the temperature rises, and indeed for disturbances whose wavelength is longer than the average interelectron separation ($\sim 1/k_F$), increased T serves to decrease screening. The electron is affected by long-wavelength disturbances more clearly and hence these renormalize the energy more effectively than at $T=0$. However, for phonons whose wavelength is small compared with the interelectron spacing, screening actually increases with temperature. At $T=0$ other electrons are apparently "frozen out" of the region immediately surrounding a given electron. As thermal effects set in the other electrons penetrate this region so that very short wavelengths are screened better at nonzero temperatures. For low densities, long-wavelength screening is a more sensitive function of temperature than for high densities. Since this is the "normal" q region where screening decreases with increasing T we find that at low densities the self-energy monatonically decreases (increases in magnitude) with increasing T. At somewhat higher densities the short-wavelength antiscreening behavior is sufficient to overcome a less sensitive screening increase at long wavelengths and even produce a weak maximum in the self-energy at nonzero temperatures, as in Fig. 4. Both screening and antiscreening effects are present for all self-energies, since we integrate over all wave vectors.

Which effect will dominate depends on which phonon q region is making the dominant contribution to the self-energy.

For polaron *holes* the phonon cloud is much more compact. Consequently, the dominant contribution to the self-energy comes from shorter-wavelength phonons than in the electron case. Since it is this region where screening increases with T, we expect the hole self-energies to exhibit more antiscreening throughout the range of temperatures. This is precisely what we see in Fig. 5, where the hole self-energies do not approach their unscreened limit (≈ 10 meV) with increasing temperature as quickly as the electrons do in Fig. 4. Figure 5(a) is for zero thickness; Fig. 5(b) is for 200 Å.

D. Effective mass

The effect of temperature-dependent screening on the effective mass can be explained in the same terms in which we understand the behavior of the polaron self-energy. In both cases, the electron-phonon coupling is reduced by finite well width and also by screening. Equation (2.9) gives the two-dimensional, zero screening limit of m^*. In the limit of infinite screening ($\epsilon \to \infty$) the electron no longer couples to the phonon at all and we recover $m^* = m$. Thus, m^* is bounded between 0.067 and 0.0689 (in units of the free-electron mass). For purposes of comparison, the three-dimensional effective mass in the zero screening limit is given by

$$\frac{1}{m^*} = \frac{1}{m}\left[1 - \frac{\alpha}{6}\right] \to m^* = m(1+\alpha/6) . \tag{4.1}$$

The most significant result in Fig. 6 is simply the overall magnitude of the change in m^* with changing T. We find that m^* changes by less than 1% over the whole temperature range (0–300 K) in the zero well thickness limit shown in Fig. 6(a). In Fig. 6 we also

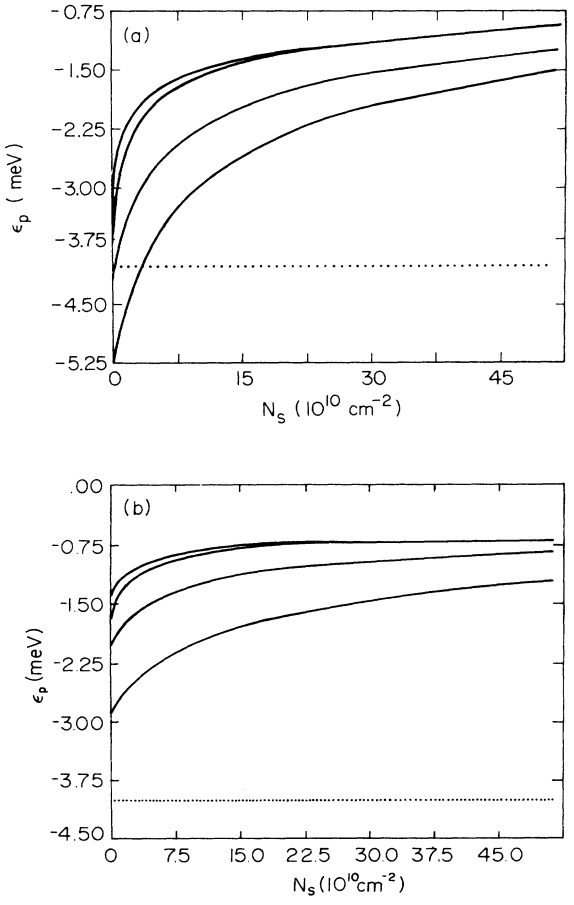

FIG. 3. Polaronic corrections to the conduction-band edge as a function of electron density for a variety of temperatures, from top to bottom: 0, 10, 150, and 300 K. The horizontal dotted line is the unscreened limit for $T=0$ K. (a) shows the corrections for the strictly two-dimensional zero-well-width limit. (b) shows the corrections for a 200-Å well. (All results are perturbative.)

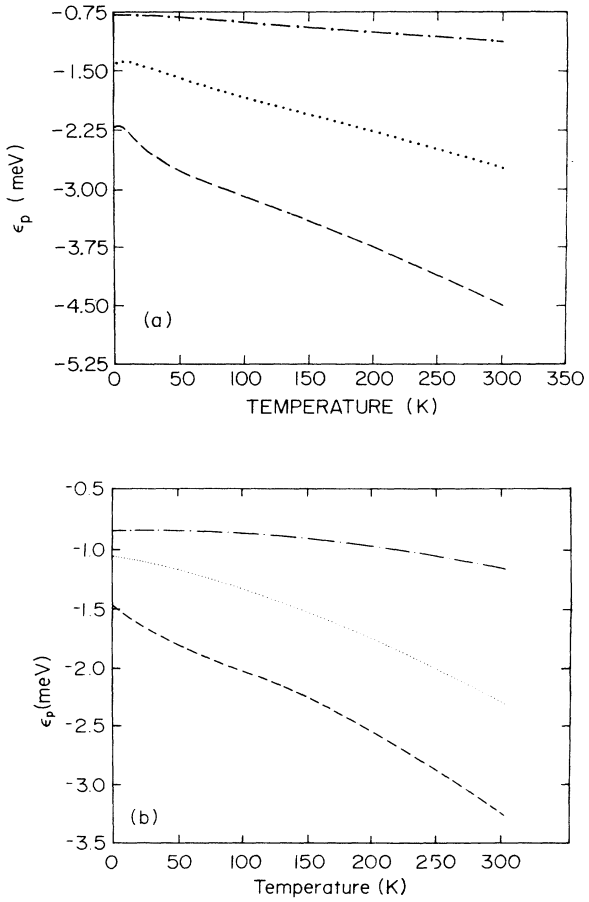

FIG. 4. Polaronic corrections to the conduction-band edge as a function of temperature for a variety of electron densities. From bottom to top: 1.6, 12.8, and 100.0×10^{10} electrons/cm^2. (a) shows the corrections for the strictly two-dimensional zero-well-width limit. (b) shows the correction for a 100-Å well (perturbative).

reproduce the effective-mass data from recent cyclotron resonance experiments of Brummell *et al.*[4] Evidently our calculated temperature dependence is at best a factor of 5 too small by comparison. In addition to the static RPA screening curves, Fig. 6 also shows the effective mass as calculated with static RPA screening employing classical statistics.[16] Aside from a slight overall shift in the effective mass, the curves are almost identical to those using quantum statistics. In Fig. 6(b) we include the form factor for a 170-Å well width (the experimental value). Not only does this not improve the situation, but the temperature dependence in the finite thickness case is even smaller than the zero thickness limit. While the comparison is instructive, the failure of our theory to generate the correct temperature dependence is not surprising. There is as yet no adequate theory of screening of the electron–LO-phonon coupling in high magnetic fields for two-dimensional systems. The singular nature of the density of states in two dimensions brought about by the quantization into Landau levels in high magnetic fields makes the problem very difficult to approach. In any event, the zero-field results presented here are clearly much too small to account for experiment.

In Fig. 7 we present the effective mass calculated with our final two approximations for screening: the long-wavelength limits of both static RPA with quantum statistics and static RPA with classical statistics. This last approximation[16] is the simple Debye theory for high-temperature, long-wavelength classical screening:

$$\epsilon(q,T)=1+\frac{q_D(T)}{q} ,$$

where

$$q_D(T)=q_s T_F/T=\frac{q_s k_F^2}{2m_{\pm}k_B T} . \tag{4.2}$$

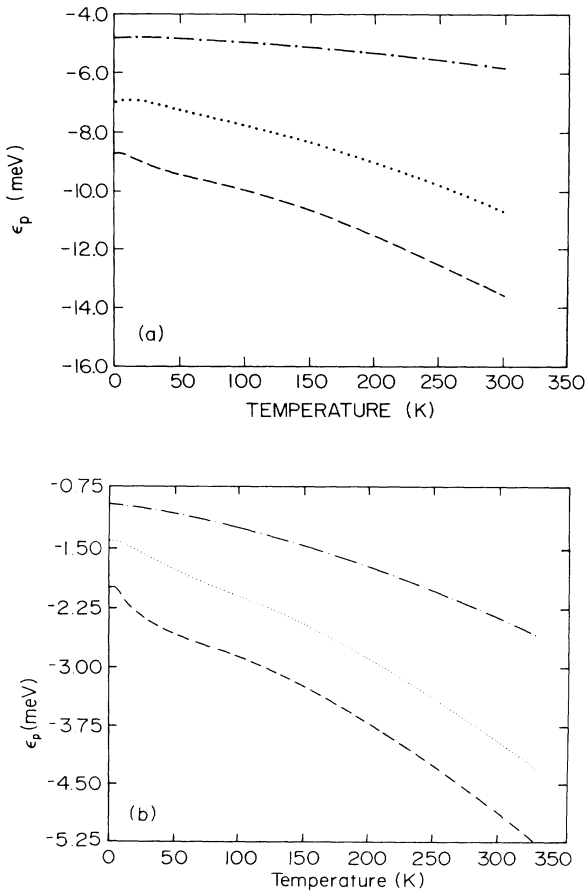

FIG. 5. Polaronic corrections to the valence-band edge as a function of temperature for a variety of hole densities, from bottom to top: 1.6, 12.8, and 100.0×10^{10} holes/cm^2. (a) shows the corrections for the strictly two-dimensional zero-well-width limit. (b) shows the corrections for a 200-Å well (perturbative).

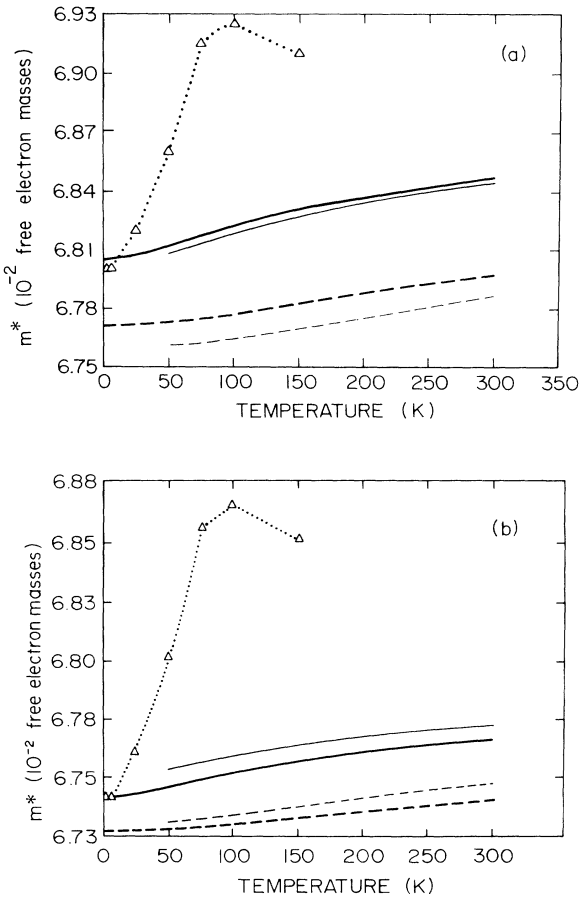

FIG. 6. Polaron effective mass as a function of temperature. The thick dashed and solid lines are for full static RPA screening with electron densities of 6×10^{11} electrons/cm^2 and 1.4×10^{11} electrons/cm^2, respectively. The thin dashed and solid lines are for classical screening for the same densities, respectively. (a) shows the effective masses in the strictly two-dimensional zero-well-width limit. (b) shows the effective massed for a 170-Å well. The triangles are experimental points from cyclotron resonance measurements of Ref. 4. For purposes of comparison, these data have been normalized to the zero-temperature effective mass of the full static RPA screening calculation for each of the two well widths.

This final approximation is the only one that reproduces the order of magnitude of the effective-mass temperature dependence. Again, however, the magnitude of the temperature dependence is somewhat greater in the zero-well-thickness limit [Fig. 7(a)] than in the 170-Å experimental thickness case [Fig. 7(b)].

While we cannot say that the system, in any sense, is classical at the experimental temperatures *(far from it)*, still, the fact that long-wavelength classical screening changes the effective mass by the correct order of magnitude is not very surprising. In the zero-field case screening is limited by the amount of available phase space for pair creation by phonons. Electrons far below the Fermi sea (at zero temperature, say) cannot participate in screening because the nearest available states are too far away. Therefore, screening is due predominantly to electrons within $k_B T$ of the Fermi surface. In a strong magnetic field in two dimensions, each Landau level has a degeneracy of order $g \approx 1/2\pi l^2$, where l is the radius of the ground orbit, given by $l^2 = c/eH$.[8] For $H = 100$ kOe, for example, $l = 81$ Å and $g = 2.5 \times 10^{11}$ cm^{-2}. These are nearly *all* the electrons for the kind of densities we are considering. Therefore, just as in the classical case where no transitions at all are prohibited by statistics, the strong magnetic field leaves each electron the same amount of phase space to scatter into. Just what the structure of the energy levels in this phase space is, and how that affects screening in detail, awaits a more complete theory of screening in a strong magnetic field including full effects of level broadening which is crucial[17] in getting nonsingular results at high magnetic fields.

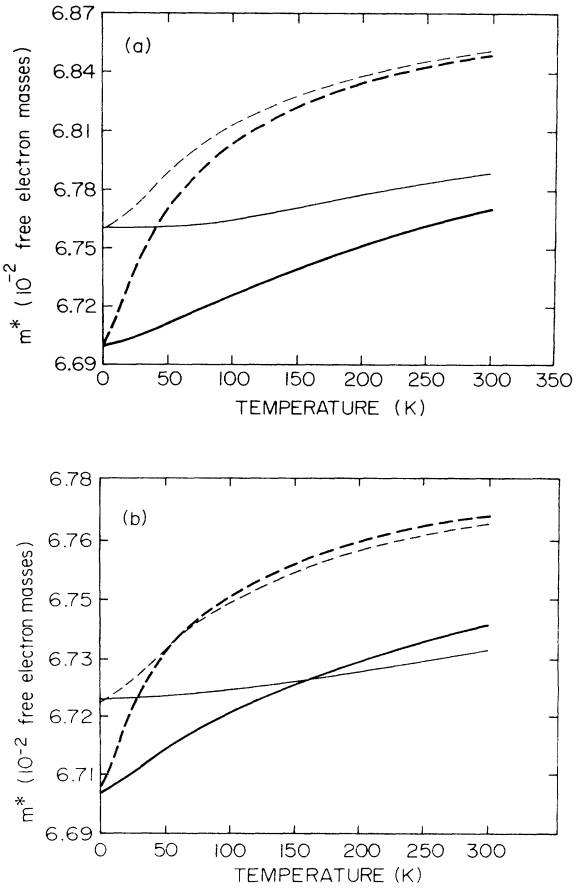

FIG. 7. Polaron effective mass as a function of temperature in the long-wavelength limit. The thin solid and dashed curves are for the $q = 0$ limit of static RPA screening at 6×10^{11} electrons/cm^2 and 1.4×10^{11} electrons/cm^2, respectively. The thick solid and dashed curves are for the $q = 0$ limit of classical screening for the same densities, respectively. (a) shows the effective masses for the strictly two-dimensional zero-well-width limit. (b) shows the effective masses for a 170-Å well.

V. CONCLUSION

The polaron self-energy in a two-dimensional GaAs quantum well is comparable in magnitude to exchange correlation effects on the electron energy. This coupling of the electrons to LO phonons works to shrink the gap between the conduction and valence bands. Screening and finite well thickness weaken the electron-phonon coupling and so counter-renormalize the band gap. Screening increases uniformly with free-carrier density but has a complex dependence on temperature and phonon wavelength. Screening of long-wavelength phonons decreases as T increases, but phonons within the interparticle distance are not maximally screened at $T = 0$.

We have presented calculations of the polaron energies using both a perturbative approach and a variational calculation. The perturbative approach employs static screening and the variational calculation employs a more complete dynamical screening model. We compared the methods of calculation and found that static screening overestimates screening.

We used the perturbative polaron energy to derive a formula for the polaron effective mass. The variation of the effective mass with temperature resulted from the temperature dependence of screening and showed the same effects as the polaronic energy. The temperature dependence of our static Thomas-Fermi screening was not sufficient to reproduce the measured temperature dependence of the effective mass. Our overall temperature dependence was too small by a factor of 5. A calculation using long-wavelength classical screening produced an effective mass whose temperature dependence was the right order of magnitude. We explained this result as a consequence of the extreme degeneracy of two-dimensional electronic systems in a strong magnetic field. Nonetheless, we noted that anything more than a passing resemblance to the effective-mass data will require a more sophisticated theory of electron-phonon screening in a high magnetic field in two dimensions, which is unavailable at the present time.

ACKNOWLEDGMENTS

We would like to thank the U.S. Army Research Office for their support in this research. The work has also been supported by the U.S. Department of Defense.

[1]S. Das Sarma, Phys. Rev. B **27**, 2590 (1983). For a recent review of polarons in two-dimensional systems, see U. Merkt, M. Horst, and J. P. Kotthaus, Phys. Scr. **T13**, 272 (1986), and references therein.
[2]D. A. Kleinman and R. C. Miller, Phys. Rev. B **32**, 2266 (1985).
[3]S. Das Sarma and B. A. Mason, Phys. Rev. B **31**, 5536 (1985).
[4]M. A. Brummell, R. J. Nicholas, M. A. Hopkins, J. J. Harris, and C. T. Foxon, Phys. Rev. Lett. **58**, 77 (1987).
[5]S. Das Sarma and B. A. Mason, Ann. Phys. (N.Y.) **163**, 78 (1985).
[6]T. Ando, A. B. Fowler, and F. Stern, Rev. Mod. Phys. **54**, 437 (1982).
[7]F. Stern and S. Das Sarma, Phys. Rev. B **30**, 840 (1984).
[8]L. F. Lemmens, J. T. Devreese, and F. Brosens, Phys. Status Solidi **82**, 439 (1977).
[9]S. Das Sarma, Phys. Rev. B **33**, 5401 (1986); P. Maldague, Surf. Sci. **73**, 296 (1978).
[10]S. Das Sarma and B. A. Mason, Phys. Rev. B **31**, 1177 (1985).
[11]W. Xiaoguang, F. M. Peeters, and J. T. Devreese, Phys. Status Solidi B **133**, 229 (1986).
[12]M. L. Glasser, J. Phys. C **10**, L121 (1977).
[13]A. Czachor, A. Holas, S. R. Sharma, and K. S. Singwi, Phys. Rev. B **25**, 2144 (1982).
[14]F. Stern, Phys. Rev. Lett. **18**, 546 (1967).
[15]B. Vinter, Phys. Rev. B **13**, 4447 (1976); S. Das Sarma, R. K. Kalia, M. Nakayama, and J. J. Quinn, *ibid.* **19**, 6397 (1979).
[16]A. L. Fetter, Phys. Rev. B **10**, 3739 (1974).
[17]S. Das Sarma, Solid State Commun. **36**, 357 (1980).